IEEE Access
Multidisciplinary | Rapid Review | Open Access Journal

Received October 9, 2019, accepted October 23, 2019, date of publication October 30, 2019, date of current version November 15, 2019.

Digital Object Identifier 10.1109/ACCESS.2019.2950531

A Robust Filtering Method for X-Ray Pulsar Navigation in the Situation of Strong Noises and Large State Model Errors

LIRONG SHEN, HAIFENG SUN, XIAOPING LI, YANMING LIU, HAIYAN FANG, JIANYU SU, AND LI ZHANG

[1]School of Aerospace Science and Technology, Xidian University, Xi'an 710071, China
[2]Key Laboratory of Information and Structure Efficiency in Extreme Environment, Ministry of Education of China, Xidian University, Xi'an 710071, China

Corresponding author: Haifeng Sun (hfsun@xidian.edu.cn)

This work was supported in part by the National Key Research and Development Program of China under Grant 2017YFB0503300, in part by the Chinese National Natural Science Foundation under Grant 61627901, in part by the National Natural Science Foundation of China under Grant 61603287, Grant 61502373, and Grant 61771371, and in part by the Initial Scientific Research Fund of Young Teacher in Xidian University under Grant 20103196787.

ABSTRACT X-ray pulsar-based navigation (XPNAV) is one of the perfect ways for autonomous deep-space navigation in the future. Due to spacecraft state model errors and strong cosmic background noises, low navigation accuracy is one of the main problems in XPNAV. This paper proposes a robust navigation filtering method to reduce the serious effect of spacecraft state model errors and strong noises on XPNAV. This method uses state model errors and pulsar observation errors to estimate and correct the state model. And then, to predict the spacecraft' state in the next moment with high precision, the gain matrix is adjusted in quasi real-time by using the fading factor to ensure a minimized state estimation error variance in the next moment and an orthogonal residual sequence at different times. Finally, experimental results of multi-group simulations show that the proposed method had significantly improved navigation accuracy. And the accuracy of the proposed method is better than that of H∞ robust filter and STUKF, especially when the state model errors and noise are great. Under the same conditions, compared with the other two methods, the proposed method has the minimum navigation filtering error and the strongest robustness.

INDEX TERMS State model error, strong noise, X-ray pulsar-based navigation, robustness.

I. INTRODUCTION

Pulsars are rapidly rotating neutron stars that emit signals with a stable period [1]. Pulsar signals radiating in the X-ray band of the electromagnetic spectrum can be easily recorded by miniaturized X-ray detectors installed on spacecraft [2]. As a novel autonomous navigation method, the X-ray pulsar-based navigation (XPNAV) is available to provide position, velocity, attitude, and timing information for vehicles travelling near the Earth, into deep space, or on interplanetary missions, and has been extensively researched in recent years [3]–[14].

The basic observations in XPNAV are pulse time-of-arrivals (TOAs), which is determined by comparing the integrated pulse profile at the spacecraft with the standard pulse profile at the solar system barycenter (SSB) [1]–[3]. The orbit of a spacecraft can therefore be estimated by combining the equations of orbital dynamics and pulsar observations [4]. However, the forces acting on a spacecraft are complex. And the orbital dynamic model has errors and uncertainties. In addition, the noise and discontinuity of observations also degrade navigation accuracy seriously.

A feasible and effective strategy for resolving the above problem is to combine navigation filtering with the orbital dynamics equation and pulsar measurements to realize autonomous navigation of the spacecraft. The navigation filtering method is thus critical in XPNAV.

In XPNAV, the extended Kalman filter (EKF) is often applied to state estimation of spacecraft and has low computational complexity and fast calculation speed. However, EKF applies a first-order linearization truncation to Taylor's expansion of the nonlinear model and ignores other higher-order terms. It will lead to state model errors and reduce the precision of navigation. Moreover, EKF requires a Jacobian matrix whose calculation is complicated [15]–[17]. The unscented Kalman filter (UKF) uses deterministic sampling to approximate the probability density of spacecraft' states and estimates the mean and covariance without requiring

The associate editor coordinating the review of this manuscript and approving it for publication was Xudong Zhao.

the Jacobian matrix to be solved [18]–[20], which is helpful to improve the accuracy of XPNAV. However, the filtering precision and robustness of UKF will greatly reduce when noises, interference and large model errors exist.[21]. To improve the accuracy of XPNAV, the strong tracking unscented Kalman filter (STUKF) [22] uses a fading factor to control gain matrix and forces the residual sequences to be orthogonal. Thus, the STUKF has good robustness against noises and interferences. However, large model errors and the incompletely orthogonal residual sequences will lead to large navigation errors in XPNAV. Recent years, an improved strong tracking SVD-UKF [23] was researched in which multiple fading factor matrices are introduced to realize the strong tracking of the state. An H∞ filter [24]–[26] was used to the CNS/Pulsar integrated navigation due to its robustness to colored noise. A modified unscented Kalman filter (MUKF) was researched to handle the situation where the process and measurement noises are correlative [8]. And a modified square-root unscented Kalman filter (MSUKF) was researched to handle with the problems arisen from the special properties of interplanetary vehicles and employs a fading factor to reduce the impact of modeling error on the proposed navigation system [27]. The above methods can improve navigation accuracy and have good robustness for each problem studied. However, due to lack of estimation and modification of the spacecraft' state model errors, the navigation accuracy will decrease when the state model errors are large. In order to improve measurement model accuracy and reduce model parameter identification error, a robust multiple model adaptive estimation (RMMAE) method was proposed with different measurement models being utilized to satisfy the filter's true statistical information [28]. This method can suppress model parameter identification error. However, as the probability of the best model tends to 1 while the others are 0, which will cause new observations to be ignored by the filter. In addition, the more the model is set, the more accurate the uncertainty of the system model parameters will be described. But the complex parallel filtering structure will increase the calculation amount and the cost of XPNAV.

In this paper, a nonlinear predictive strong tracking unscented Kalman filter (NPSTUKF) is proposed to reduce the effect of state model errors and high levels of noises on the accuracy of the orbit determination in XPNAV. This method uses state model errors and observation errors to construct a criterion function of state model error. By minimizing the criterion function, the system state model errors can be estimated. And the system state model can be corrected using the minimum state model error. Then, to predict the spacecraft' state of the next moment with high precision, the gain matrix is adjusted in quasi real-time by using the fading factor to ensure a minimized variance of the state estimation error and an orthogonal residual sequence at different times. Finally, for verifying the robustness and effectiveness of the proposed method, we compared it with STUKF and H∞ robust filter in the situations of a normal situation, strong noise, and in the presence of state model errors. Experimental results of multi-group simulations show that the proposed method can significantly improve the accuracy of position and velocity estimation without increasing the computational complexity. And the accuracy of the proposed method is better than that of the STUKF and the H∞ robust filter, especially when the state model errors and noise are great.

This paper is organized as follows. Section 2 gives the model of XPNAV system. Section 3 designs NPSTUKF-based navigation in detail. Section 4 tests the effectiveness of the proposed method in the presence of noises and state model errors in simulations. Section 5 draws conclusions from the simulation results.

II. MODEL OF XPNAV SYSTEM

A. XPNAV MEASUREMENT MODEL

The measurement of XPNAV is the difference between the pulse TOA at the SSB, t_{SSB}, which can be predicted by the pulse timing model, and the corresponding pulse TOA at the spacecraft, t_{SC}, which can be calculated at the end of an observation period for a pulsar providing weak pulsed signal [27]. To obtain pulse TOA accurately in XPNAV, measurements must be made relative to the inertial frame of the SSB, which is an unaccelerated frame with respect to pulsars. Thus, a time transformation from the spacecraft to the SSB is needed. Sources of time delay, including the Roemer, Einstein, and Shapiro delays, should be considered. The transformation of the photon arrival time from the spacecraft to the SSB [3] can thus be expressed as

$$\begin{aligned} t_{SSB} = t_{SC} &+ \frac{1}{c}\boldsymbol{n}\cdot\boldsymbol{r} \\ &+ \frac{1}{2cD_0}[(\boldsymbol{n}\cdot\boldsymbol{r})^2 - r^2 + 2(\boldsymbol{n}\cdot\boldsymbol{b})(\boldsymbol{n}\cdot\boldsymbol{r}) - 2(\boldsymbol{b}\cdot\boldsymbol{r})] \\ &+ \frac{2\mu_s}{c^3}\ln\left|\frac{\boldsymbol{n}\cdot\boldsymbol{r} + \boldsymbol{n}\cdot\boldsymbol{b} + \|\boldsymbol{r}+\boldsymbol{b}\|}{\boldsymbol{n}\cdot\boldsymbol{b} + b}\right| \end{aligned} \tag{1}$$

where $\boldsymbol{n} = [\cos(\beta)\cos(\alpha) \quad \cos(\beta)\sin(\alpha) \quad \sin(\beta)]^{\mathrm{T}}$ is the unit direction vector of the pulsar with respect to the SSB obtained using the right ascension α and declination β of the pulsar, c is the speed of light, D_0 is the range from the pulsar to the SSB, and $\boldsymbol{b}$ is the position vector of the Sun with respect to the SSB. The second term on the right-hand side of (1) is the first-order Doppler delay. The third term relates to the effect of annual parallax. The fourth term is the Shapiro delay effect. $\boldsymbol{r}$ is the position vector of the spacecraft, expressed as

$$\boldsymbol{r} = \boldsymbol{r}_E + \boldsymbol{r}_{SC/E} \tag{2}$$

$\boldsymbol{r}_E$ is the position of the Earth, and $\boldsymbol{r}_{SC/E}$ is the position vector of spacecraft with respect to Earth.

The absolute distance between the spacecraft and SSB along the direction of the ith pulsar can be expressed as

$$\begin{aligned} &\Delta R_i \\ &= c\cdot(t^i_{SSB} - t^i_{SC}) \\ &= \boldsymbol{n}_i\cdot\boldsymbol{r} + \frac{1}{2D_0}[(\boldsymbol{n}_i\cdot\boldsymbol{r})^2 - r^2 + 2(\boldsymbol{n}_i\cdot\boldsymbol{b})(\boldsymbol{n}_i\cdot\boldsymbol{r}) - 2(\boldsymbol{b}\cdot\boldsymbol{r})] \end{aligned}$$

$$+\frac{2\mu_s}{c^2}\ln\left|\frac{\boldsymbol{n}_i\cdot\boldsymbol{r}+\boldsymbol{n}_i\cdot\boldsymbol{b}+\|\boldsymbol{r}+\boldsymbol{b}\|}{\boldsymbol{n}_i\cdot\boldsymbol{b}+b}\right| \tag{3}$$

In general, the Shapiro delay of the Sun introduces a time difference of arrival (TDOA) measurement error of less than 10 μs. The parallax term introduces a TDOA measurement error of about 0.1 μs. Thus, the navigation errors caused by Shapiro delay of the Sun and parallax term are very small in estimating the position and velocity information of the spacecraft.

Considering the relativistic effects, the spatial geometric effect, and ignoring the delay effect of parallax and Shapiro delay of the Sun alone, this paper uses the offset of TOAs from the corresponding pulsar to the SSB and to the spacecraft to describe the absolute distance between the spacecraft and SSB along the direction of the ith pulsar:

$$\Delta R_i = \boldsymbol{n}_i^{\mathrm{T}}\boldsymbol{r} = c(t_{SSB}^i - t_{SC}^i) \tag{4}$$

And the measurement model of XPNAV is

$$\boldsymbol{Y} = \Delta\boldsymbol{R} + \boldsymbol{\zeta} = \boldsymbol{H}\boldsymbol{X} + \boldsymbol{\zeta} \tag{5}$$

where $\boldsymbol{Y} = [y^{(1)}, y^{(2)}, \ldots, y^{(N)}]^{\mathrm{T}}$, N is the number of the pulsars selected, $\boldsymbol{H} = [\boldsymbol{n}_{N\times 3}\boldsymbol{0}_{N\times 3}]$ is the measurement matrix, $\boldsymbol{X}(t) = [x\ y\ z\ v_x\ v_y\ v_z]^{\mathrm{T}}$. $\boldsymbol{\zeta}$ is the measurement noise matrix, including the higher-order term of the measurement model of XPNAV, which can be modeled as zero-mean Gaussian white noise with standard variance σ_r, expressed as

$$\sigma_r = c\cdot\frac{W\sqrt{[B_X + F_X(1-p_f)]d + F_X p_f}}{2F_X p_f\sqrt{AT_{obs}}} \tag{6}$$

where W is the width of the pulse, c is the speed of light, B_X is the X-ray background radiation flux, and F_X is the radiation photon flux from the X-ray pulsar. p_f is the ratio of the pulse radiation flux to the average radiation flux in a pulse period, d is the ratio of the pulse width to the pulse period, A is the area of X-ray detector, and T_{obs} is the observational period of pulsar signals.

B. ORBIT DYNAMIC MODEL FOR XPNAV

This paper estimates the state vector of the spacecraft's position and velocity in the J2000.0 Earth Centered Inertial coordinate system, only considering Earth's central gravity and J2 perturbation. The state vector of the spacecraft is expressed as

$$\mathbf{X}(t) = [x\ y\ z\ v_x\ v_y\ v_z]^{\mathrm{T}} \tag{7}$$

The orbit dynamic model of the spacecraft is modeled as

$$\dot{\boldsymbol{X}}(t) = \begin{bmatrix}\boldsymbol{v}\\ \boldsymbol{a}\end{bmatrix} = f(\boldsymbol{X}(t)) + \boldsymbol{w}(t)$$
$$= \begin{Bmatrix} v_x \\ v_y \\ v_z \\ -\mu\frac{x}{r^3}[1 - J_2(\frac{R_e}{r})^2(7.5\frac{z^2}{r^2} - 1.5)] \\ -\mu\frac{y}{r^3}[1 - J_2(\frac{R_e}{r})^2(7.5\frac{z^2}{r^2} - 1.5)] \\ -\mu\frac{z}{r^3}[1 - J_2(\frac{R_e}{r})^2(7.5\frac{z^2}{r^2} - 4.5)] \end{Bmatrix} + \boldsymbol{w}(t) \tag{8}$$

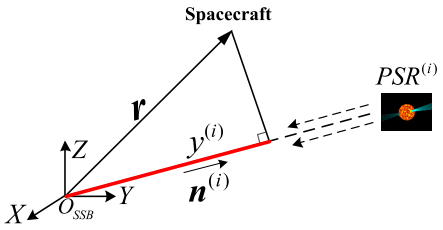

FIGURE 1. Principle of XPNAV.

where $\dot{\boldsymbol{X}}(t)$ is the derivative of $\mathbf{X}(t)$, μ is the gravitational constant of the Earth, R_e is the radius of the Earth, and r is the spacecraft's position relative to the Earth. J2 is the nonspherical zonal harmonic coefficient of the Earth. $\boldsymbol{w}(t)$ is the state model error, which comprises unmodeled terms and higher-order terms of other perturbation acceleration.

III. NAVIGATION BASED ON NPSTUKF

A. MAIN BASIS OF THE NPSTUKF METHOD

For improve the precision of XPNAV, based on the UKF, this paper proposes a NPSTUKF method by combining the advantages of the nonlinear prediction theory and strong tracking theory to reduce the serious effects of the state model errors and high levels of noises on orbit determination in XPNAV. On the one hand, the proposed method has the ability to estimate and correct the state model error of spacecraft. On the other hand, a fading factor is introduced to realize the quasi real-time adjustment of gain matrix and can ensure the convergence of the navigation filter. Thus, the proposed method can improve the precision of XPNAV. The main ideas behind the propose method are shown in Fig.2.

B. XPNAV BASED ON THE NPSTUKF

Suppose the state model and the observation model of XPNAV system are estimated as

$$\begin{cases}\dot{\widehat{\boldsymbol{X}}} = \boldsymbol{f}\left(\widehat{\boldsymbol{X}}(t)\right) + \boldsymbol{U}\cdot\widehat{\boldsymbol{A}}(t)\\ \widehat{\boldsymbol{Y}}(t) = \boldsymbol{h}\left(\widehat{\boldsymbol{X}}(t)\right) + \boldsymbol{\zeta}(t)\end{cases} \tag{9}$$

where $\dot{\widehat{\boldsymbol{X}}} \in \boldsymbol{R}^n$ and $\widehat{\boldsymbol{Y}} \in \boldsymbol{R}^m$ are respectively the estimated values of state vector and observation vector. $\boldsymbol{f}(\cdot)$ and $\boldsymbol{h}(\cdot)$ are nonlinear functions. $\widehat{\boldsymbol{A}}(t) \in \boldsymbol{R}^{p\times 1}$ represents the estimated value of the state model errors. $\boldsymbol{U} \in \boldsymbol{R}^{n\times p}$ is the input matrix. In this paper, the system state model errors are mainly due to the unmodeled high-order perturbation forces which affect the acceleration terms. Thus, set $\boldsymbol{U} = [\boldsymbol{0}_{3\times 3}\ \boldsymbol{1}_{3\times 3}]^{\mathrm{T}}$. $\zeta(t)$ is the observation noise with $E[\zeta(t_k)] = 0$ and $\sigma_\zeta^2 = \boldsymbol{R}_k$. The correlation coefficient $\gamma_{\zeta_k,\zeta_j} = \boldsymbol{R}_k\delta_{kj}$,

$$\delta_{kj} = \begin{cases}1, & k = j\\ 0, & k \neq j\end{cases} \tag{10}$$

Firstly, we set the initial value of the spacecraft' state vector $\boldsymbol{X}_0$, covariance $\boldsymbol{P}_0$ and the initial state model error $\widehat{\boldsymbol{A}}_0$. Determine the system noise covariance $\boldsymbol{Q}$. Calculate the pulse TOA

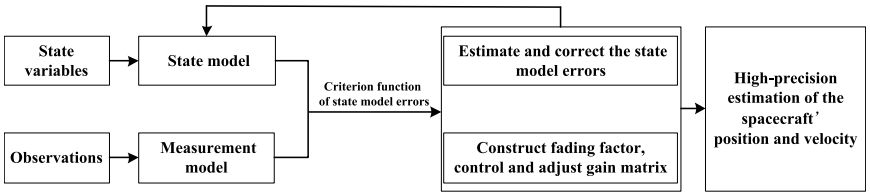

FIGURE 2. Main ideas behind the NPSTUKF method.

estimation error $\boldsymbol{\sigma}_{TOA}$ and the distance measurement error $\boldsymbol{\sigma}_r = c \cdot \boldsymbol{\sigma}_{TOA}$. Determine the observation error covariance $\boldsymbol{R} = diag(\sigma_{r1}^2, \sigma_{r2}^2 \ldots, \sigma_{rn}^2)$.And set the observation cycle and filtering cycle of the navigation.

In this paper, by adopting the symmetric sampling strategy, the sigma points $\widehat{\boldsymbol{X}}_k$ can be selected in accordance with

$$\begin{cases} \boldsymbol{X}_{0,k} = \widehat{\boldsymbol{X}}_k \\ \boldsymbol{X}_{i,k} = \widehat{\boldsymbol{X}}_k + \sqrt{(n+\lambda)} \cdot (\text{chol}\{\boldsymbol{P}_k\})_i \\ \boldsymbol{X}_{i+n,k} = \widehat{\boldsymbol{X}}_k - \sqrt{(n+\lambda)} \cdot (\text{chol}\{\boldsymbol{P}_k\})_i \quad i = 1, 2, \ldots n \end{cases} \tag{11}$$

where n is the number of components in the state vector. $\lambda = \alpha^2(n+K) - n$, with $0 \leq \alpha \leq 1$. $(\text{chol}\{\boldsymbol{P}_k\})_i$ denotes the ith column of the down triangular matrix after cholesky decomposition for matrix $\boldsymbol{P}_k$. The weights W_m and W_c are determined as

$$\begin{cases} W_m^{(0)} = \dfrac{\lambda}{n+\lambda} \\ W_c^{(0)} = \dfrac{\lambda}{n+\lambda} + (1 - \alpha^2 + \beta) \\ W_m^{(i)} = W_c^{(i)} = \dfrac{\lambda}{2(n+\lambda)} \quad i = 1, 2, \ldots 2n \end{cases} \tag{12}$$

where β is a parameter associated with prior information of the state. Generally set $\beta = 2$.

Here, the discrete forms of the state model and the observation model of XPNAV system can be written as

$$\begin{cases} \dot{\widehat{\boldsymbol{X}}} = \boldsymbol{f}\left(\widehat{\boldsymbol{X}}(t_k)\right) + \boldsymbol{U} \cdot \widehat{\boldsymbol{A}}(t_k) \\ \widehat{\boldsymbol{Y}}(t_k) = \boldsymbol{h}\left(\widehat{\boldsymbol{X}}(t_k)\right) + \boldsymbol{\zeta}(t_k) \end{cases} \tag{13}$$

For accurately estimating and updating the state of spacecraft, it is necessary to estimate the state model errors of spacecraft. In this paper, the state model errors investigated mainly come from the acceleration items corresponding to the unmodeled high-order perturbation force. Thus, according to the model presented as (13), we need to take the derivative of $\boldsymbol{h}(\widehat{\boldsymbol{X}}(t_k))$ twice along the vector field $\boldsymbol{f}(\widehat{\boldsymbol{X}}(t_k))$ to show any acceleration component in the state model errors. Here, the Lie derivative is used, which is defined as

$$\begin{aligned} L_f h(x) &= \nabla h(x) \cdot f(x) = \frac{\partial h(x)}{\partial x} \cdot f(x) \\ &= \left(\frac{\partial h(x)}{\partial x_1}, \frac{\partial h(x)}{\partial x_2}, \frac{\partial h(x)}{\partial x_3} \ldots \frac{\partial h(x)}{\partial x_n}\right) \cdot f(x) \\ &= dh(x) \cdot f(x) = \sum_{i=1}^{n} \frac{\partial h(x)}{\partial x_i} \cdot f_i(x) \end{aligned} \tag{14}$$

And multiple Lie derivatives are defined as

$$L_f^k h(x) = L_f(L_f^{k-1} h(x)) = \frac{\partial (L_f^{k-1} h(x))}{\partial x} \cdot f(x) \tag{15}$$

where $L_f^0 h(x) = h(x)$ denotes that no derivative is taken. In this paper, we set the system relative degree $r_i = 2$.

Then, using the knowledge of the Lee derivative, the Taylor expansion of the observation equation in (13) is carried out with ignoring the higher-order terms. And the pulsar observations at $k+1$ time can be predicted using the following expression,

$$\begin{aligned} \widehat{\boldsymbol{Y}}(t_k + \Delta t) = \widehat{\boldsymbol{Y}}(t_k) + z\left(\widehat{\boldsymbol{X}}(t_k), \Delta t\right) \\ + \boldsymbol{\Lambda}(\Delta t) \boldsymbol{S}\left(\widehat{\boldsymbol{X}}(t_k)\right) \widehat{\boldsymbol{A}}(t_k) \end{aligned} \tag{16}$$

$\Delta t = t_{k+1} - t_k$ is the sampling period. $\widehat{\boldsymbol{Y}}(t_{k+1}) = \widehat{\boldsymbol{Y}}(t_k + \Delta t)$ is the predicted pulsar observation at $k+1$ time. $z(\widehat{\boldsymbol{X}}(t_k), \Delta t) \in R^{m \times 1}$ is the first order term of Taylor expansion. Its expression is [29]

$$z\left(\widehat{\boldsymbol{X}}(t_k), \Delta t\right) = \sum_{i=1}^{2} \frac{\Delta t^i}{i!} L_f^i(\boldsymbol{h}(\widehat{\boldsymbol{X}}(t_k))) \tag{17}$$

where $L_f^i(\boldsymbol{h}(\widehat{\boldsymbol{X}}(t_k)))$ is the ith-order Lie derivative of $\boldsymbol{h}(\widehat{\boldsymbol{X}}(t_k)$ about $\boldsymbol{f}(\widehat{\boldsymbol{X}}(t_k))$. $\boldsymbol{\Lambda}(\Delta t) \boldsymbol{S}\left(\widehat{\boldsymbol{X}}(t_k)\right) \widehat{\boldsymbol{A}}(t_k)$ is the second order term of Taylor expansion, where $\boldsymbol{\Lambda}(\Delta t) \in R^{m \times m}$ with its diagonal elements $\lambda_{ii} = (\Delta t)^{r_i}/(r_i!), i = 1, 2, \ldots m$. $\boldsymbol{S}(\widehat{\boldsymbol{X}}(t_k)) \in \boldsymbol{R}^{m \times q}$ with the element in each row being

$$s_i = [L_{u_1}[L_f^{r_i - 1}(h_i)] \ldots L_{u_k}[L_f^{r_i - 1}(h_i)]], \; k = 1, 2, \ldots p \tag{18}$$

$$\boldsymbol{F}_{constraint}(\widehat{\boldsymbol{A}}(t)) = \frac{\left\{\boldsymbol{Y}(t_k + \Delta t) - \widehat{\boldsymbol{Y}}(t_k + \Delta t)\right\}^{\mathrm{T}} \boldsymbol{R}^{-1} \left\{\boldsymbol{Y}(t_k + \Delta t) - \widehat{\boldsymbol{Y}}(t_k + \Delta t)\right\}^{\mathrm{T}}}{2} + \frac{\widehat{\boldsymbol{A}}(t)^T \boldsymbol{W} \widehat{\boldsymbol{A}}(t)}{2} \tag{19}$$

where $\boldsymbol{u}_k$ is the element of the kth column of matrix U.And the $L_{u_k}(L_f^{r_i-1}h_i) = (\partial L_f^{k-1}(h_i)/\partial\widehat{\boldsymbol{X}}) \cdot \boldsymbol{u}_k$.

And then, in order to estimate the state model errors, based on the weighted sum of the observation errors and the state model errors, this paper constructs a constraint function of the state model errors in (19), as shown at the bottom of the previous page.

where $\boldsymbol{Y}(t_k + \Delta t)$ denotes the observations at $k+1$ time. $\boldsymbol{W}$ is the model error weighting matrix. By taking the derivative of the constraint function $F_{constraint}(\widehat{\boldsymbol{A}}(t))$ and setting it to zero,

$$\frac{\partial F_{constraint}(\widehat{\boldsymbol{A}}(t))}{\partial\widehat{\boldsymbol{A}}(t)} = \boldsymbol{0} \tag{20}$$

this paper can obtain the estimated state model error,

$$\begin{aligned}\widehat{\boldsymbol{A}}(t) &= -\left\{\left[\boldsymbol{\Lambda}(\Delta t)\boldsymbol{S}\left(\widehat{\boldsymbol{X}}\right)\right]^{\mathrm{T}}\boldsymbol{R}^{-1}\boldsymbol{\Lambda}(\Delta t)\boldsymbol{S}\left(\widehat{\boldsymbol{X}}\right) + \boldsymbol{W}\right\}^{-1} \\ &\quad\cdot\left[\boldsymbol{\Lambda}(\Delta t)\boldsymbol{S}\left(\widehat{\boldsymbol{X}}\right)\right]\boldsymbol{R}^{-1}\left[\boldsymbol{z}\left(\widehat{\boldsymbol{X}}, \Delta t\right) - \boldsymbol{Y}(t_k+\Delta t)+\widehat{\boldsymbol{Y}}(t_k)\right]\end{aligned} \tag{21}$$

At this point, to quasi-real-time correct the state model using (21) can effectively improve the accuracy of the state model shown in (13).

Next, use the corrected state model to predict the state $\widehat{\boldsymbol{X}}_{k+1/k}$ and the state error covariance $\boldsymbol{P}_{k+1/k}$ at the next moment according to the following expression

$$\begin{aligned}\widehat{\boldsymbol{X}}_{k+1/k} &= \sum_{i=0}^{2n}\boldsymbol{W}_m^i f(\boldsymbol{X}_i) \\ \boldsymbol{P}_{k+1/k} &= \sum_{i=0}^{2n}\boldsymbol{W}_c^i\left(\boldsymbol{\chi}_i - \widehat{\boldsymbol{X}}_{k+1/k}\right)\left(\boldsymbol{\chi}_i - \widehat{\boldsymbol{X}}_{k+1/k}\right)^{\mathrm{T}} + \boldsymbol{Q}_k\end{aligned} \tag{22}$$

where $\boldsymbol{\chi}_i = \boldsymbol{f}(X_i)$

And then, calculate the sigma points $\boldsymbol{\varepsilon}_i, i = 0, 1, ...2n$ of $\widehat{\boldsymbol{X}}_{k+1/k}$ using $\widehat{\boldsymbol{X}}_{k+1/k}$ and $\boldsymbol{P}_{k+1/k}$, and predict the observations $\widehat{\boldsymbol{Y}}_{k+1/k}$ at the next moment as

$$\widehat{\boldsymbol{Y}}_{k+1/k} = \sum_{i=0}^{2n}W_m^i\boldsymbol{h}(\boldsymbol{\varepsilon}_i) \tag{23}$$

And the residual of the observations can be obtained as

$$\boldsymbol{\varsigma}_{k+1/k} = \boldsymbol{Y}_{k+1/k} - \widehat{\boldsymbol{Y}}_{k+1/k} \tag{24}$$

When the observational value of pulsar does not match the observation model, the observation error covariance will increase. If the weight of the observation value in the state estimation is not adjusted in time, the filter will diverge. Therefore, it is necessary to adjust the gain matrix in real time. And then, adjust the weights of the pulsar observations in the state estimation to ensure the convergence of the navigation filter.

Thus, in order to adjust gain matrix in real time, this paper introduced the fading factor which satisfies [30]

$$\iota_{k+1} = \begin{cases}\iota_0, & \iota_0 > 1 \\ 1, & \iota_0 \le 1\end{cases} \tag{25}$$

where l_0 is defined as

$$l_0 = \frac{\mathrm{tr}(\boldsymbol{V}_{\varsigma,k+1} - \beta_0\boldsymbol{R}_{k+1})}{\mathrm{tr}\left(\sum_{i=0}^{2n}W_c^i\left(\boldsymbol{B}_i - \widehat{\boldsymbol{Y}}_{k+1/k}\right)\left(\boldsymbol{B}_i - \widehat{\boldsymbol{Y}}_{k+1/k}\right)^{\mathrm{T}}\right)} \tag{26}$$

$\boldsymbol{B}_i = \boldsymbol{h}(\varepsilon_i)$. β_0 is the weakening factor, and $\boldsymbol{V}_{\varsigma,k+1}$ is the residual covariance of the observations, which is defined as

$$\boldsymbol{V}_{\varsigma,k+1} = \begin{cases}\varsigma(1)\varsigma(1)^{\mathrm{T}} \\ \dfrac{\rho\boldsymbol{V}_{\varsigma,k} + \varsigma(k+1)\varsigma^{\mathrm{T}}(k+1)}{1+\rho}\end{cases}, 0 < \rho \le 1 \tag{27}$$

ρ is the forgetting factor. Generally set $\rho = 0.95$.

The fading factor above is deduced from the orthogonality principle. Therefore, it can adjust the gain matrix $\mathbf{K}_{k+1}$ in real time and can ensure the following two conditions be satisfied at the same time.

$$E[(x_{k+1} - \hat{x}_{k+1})(x_{k+1} - \hat{x}_{k+1})^T] = \min \tag{28}$$

$$E(\varsigma_{k+1+j}\varsigma_{k+1}^T) = \mathbf{0}(k = 0, 1, \cdots; j = 1, 2, \cdots) \tag{29}$$

where $\hat{x}_{k+1}$ is the estimated state at $k+1$ time. min is the minimum expected on the left side of the equal sign. $\hat{x}_{k+1/k} = f(\hat{x}_k)$ is the one-step prediction of state at $k+1$ time. And $\varsigma_{k+1} = \bar{\boldsymbol{Y}}_{k+1/k} = \boldsymbol{Y}_{k+1} - \boldsymbol{h}(\hat{x}_{k+1/k})$ is the residual of the observations at $k+1$ time. (28) refers to the optimal estimation with minimum estimation error variance.(29) refers to the orthogonality of residuals at different times.

In this paper, the fading factor is introduced into the measurement covariance matrix and the cross-covariance matrix for adjusting the gain matrix in real time. Thus, the predicted observations covariance $\boldsymbol{P}_{\boldsymbol{YY},k+1}$ and the cross covariance $\boldsymbol{P}_{\boldsymbol{XY},k+1}$ adjusted by the fading factor can be obtained as follows,

$$\boldsymbol{P}_{\boldsymbol{YY},k+1} = \iota_{k+1}\sum_{i=0}^{2n}W_c^i\left(\boldsymbol{B}_i - \widehat{\boldsymbol{Y}}_{k+1/k}\right)\left(\boldsymbol{B}_i - \widehat{\boldsymbol{Y}}_{k+1/k}\right)^{\mathrm{T}} + \boldsymbol{R}_{k+1} \tag{30}$$

$$\boldsymbol{P}_{\boldsymbol{XY},k+1} = \iota_{k+1}\sum_{i=0}^{2n}W_c^i\left(\boldsymbol{\chi}_i - \widehat{\boldsymbol{X}}_{k+1/k}\right)\left(\boldsymbol{B}_i - \widehat{\boldsymbol{Y}}_{k+1/k}\right)^{\mathrm{T}} \tag{31}$$

And the gain matrix $\boldsymbol{K}_{k+1}$ can be adjusted indirectly,

$$\boldsymbol{K}_{k+1} = \boldsymbol{P}_{\boldsymbol{XY},k+1}\boldsymbol{P}_{\boldsymbol{YY},k+1}^{-1} \tag{32}$$

Finally, the spacecraft' state $\widehat{\boldsymbol{X}}_{k+1}$ and the state error covariance $\boldsymbol{P}_{k+1}$ can be estimated and updated as follows with high precision,

$$\widehat{\boldsymbol{X}}_{k+1} = \widehat{\boldsymbol{X}}_{k+1/k} + \boldsymbol{K}_{k+1}(\boldsymbol{Y}_{k+1} - \widehat{\boldsymbol{Y}}_{k+1/k}) \tag{33}$$

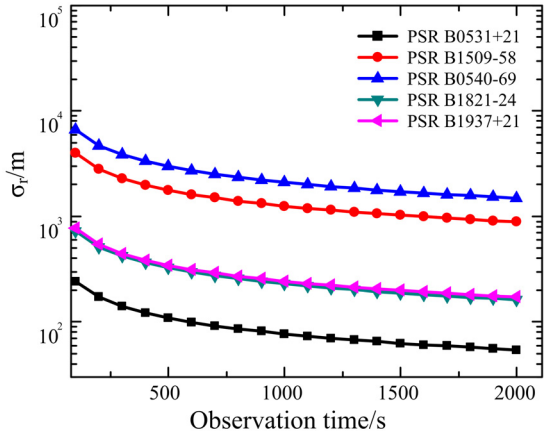

FIGURE 3. Variation in σ_r for different pulsars.

$$\boldsymbol{P}_{k+1} = \iota_{k+1}\boldsymbol{P}_{k+1/k} - \boldsymbol{K}_{k+1}\boldsymbol{P}_{\boldsymbol{YY},k+1}\boldsymbol{K}_{k+1}^{\mathrm{T}} \tag{34}$$

In summary, considering the weak X-ray pulsar signal, serious noise interferences and large state model errors, the proposed method has the ability to estimate and correct the state model error of spacecraft and to realize the quasi real-time adjustment of the gain matrix as well as to ensure the convergences of the navigation filter. Therefore, the proposed method can improve the precision of XPNAV.

IV. SIMULATIONS AND RESULTS

A. SIMULATION CONDITIONS

This section verifies the effectiveness and robustness of the proposed method for XPNAV in the J2000 Earth inertial coordinate system via some simulations. Firstly, select three navigation pulsars that have smaller ranging error σ_r from the commonly used five pulsars. σ_r can be obtained using (6). And the results are presented in Fig. 3.

Fig.3 shows that the ranging error of each pulsar decreases with increasing observation time. PSR B0531+21 [31], PSR B1821-24, and PSR B1937+21 have smaller ranging errors. Thus, these three pulsars are selected as the navigation pulsar. The parameters [32] of them are given in Table 1. The standard deviations of the ranging errors of the three pulsars are given in Table 2. Parameters in the simulation are given in Table 3.The initial states of the spacecraft are given in Table 4. The spacecraft's whole trajectory is shown in Fig.4.

In this paper, we compare the proposed method with STUKF and H∞ robust filter in the situations of a normal situation, strong noise, and in the presence of state model errors. These experiments adopt the orbital dynamics model in (8) and the observation equation of the pulsar in (5).

B. SIMULATION RESULTS

On the basis of the above experimental conditions, this paper firstly compares the performance of the proposed method with STUKF and H∞ robust filter in normal situation of weak noise. The results are presented in Fig. 5.

TABLE 1. Parameters of navigation pulsars.

Name	PSR B0531+21	PSR B1821-24	PSR B1937+21
Galactic latitude (°)	-5.78	-5.58	57.51
Galactic longitude (°)	184.56	7.80	-0.29
D(kpc)	2	5.5	3.6
α(ph/ cm^2/ s)	1.54	1.93×10^{-4}	4.99×10^{-5}
$f(1/s)$	29.9516010684378	327.4056812955600	641.9282638709569
$\dot{f}(1/s^2)$	-3.777×10^{-10}	-1.73536×10^{-13}	-4.33167×10^{-14}
$\ddot{f}(1/s^3)$	8.18×10^{-21}	5.85×10^{-30}	0

TABLE 2. Standard deviations of the ranging errors.

Name	σ_r /m($t_{obs}=300s$)
PSR B0531+21	140.69
PSR B1821-24	420.63
PSR B1937+21	444.80

TABLE 3. Parameters in the simulation.

Area of X-ray sensor	1m^2
Flux of X-ray background	0.005 ph/ cm^2/ s
Measurement period	300s
Initial state error	[10km 10km 10km 5m/s 5 m/s 5 m/s]
The initial error covariance	$\boldsymbol{P}_0$ =[10000^2 10000^2 10000^2 5^2 5^2 5^2]
Process noise covariance matrix	$\boldsymbol{Q}=diag(q_1^2,q_1^2,q_1^2,q_2^2,q_2^2,q_2^2)$, where $q_1=1m$, $q_2=0.1m/s$
Measurement noise covariance matrix	$\boldsymbol{R}=diag(\sigma_{r1}^2,\sigma_{r2}^2,\sigma_{r3}^2)$
Parameter of H∞ filter	$\theta=1\times10^{-8}$

TABLE 4. Orbit initial state of the spacecraft.

Position	X-axis	-6385277.75022981m
	Y-axis	44560765.3406456m
	Z-axis	-22339513.8328267m
Velocity	X-axis	1216.58058281597m/s
	Y-axis	1602.40144212460m/s
	Z-axis	2323.81884151026m/s

Fig 5 shown that the navigation filtering results of H∞ robust filter, STUKF, and the proposed method can converge rapidly under the large initial position and velocity errors of spacecraft. And it is noteworthy that the proposed method performs best in that it has the smallest position estimation errors. The reason is that the state model used in this paper has model errors, which will affect navigation accuracy. Among the three method, the proposed method has the ability to estimate and correct the state model errors while the other two methods do not. Thus, the navigation accuracy of H∞ robust filter and STUKF is lower than that of the proposed method.

We next analyze the XPNAV filtering performance of the proposed method in strong noise environment. In this

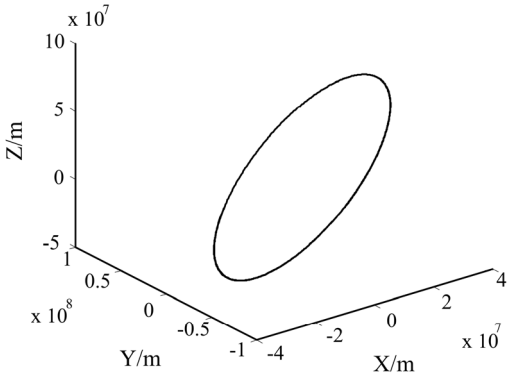

FIGURE 4. Spacecraft's whole trajectory.

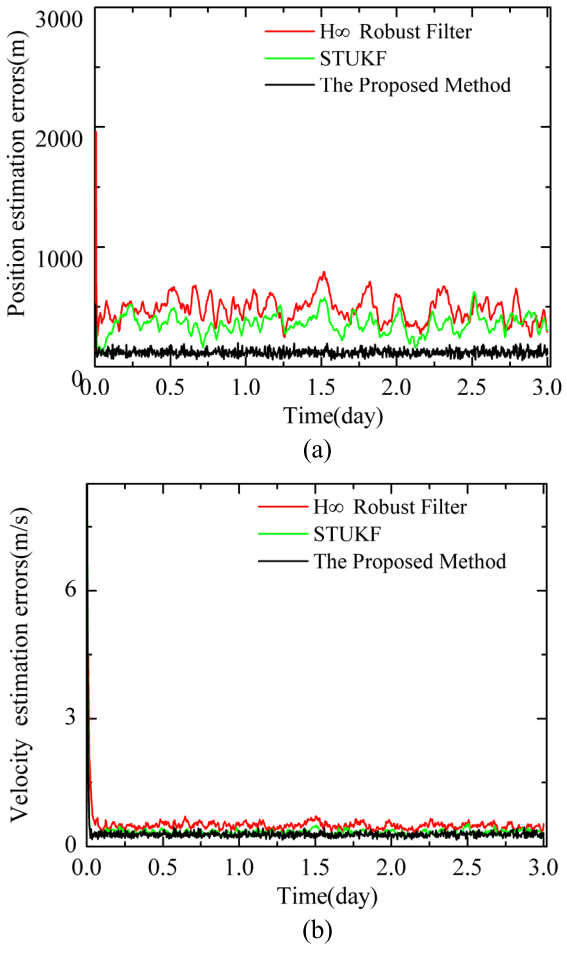

FIGURE 5. Position and velocity estimation errors in normal situation, (a) position estimation errors, (b) velocity estimation errors.

experiment, the system process noise is increased by a factor of 4, and the other conditions are unchanged. Experimental results are shown in Fig. 6.

Fig. 6 shows that the position and velocity estimation errors of H∞ robust filter and STUKF become larger in stronger noise environment. And it can be seen that strong noise has great effect on the navigation performance. In this

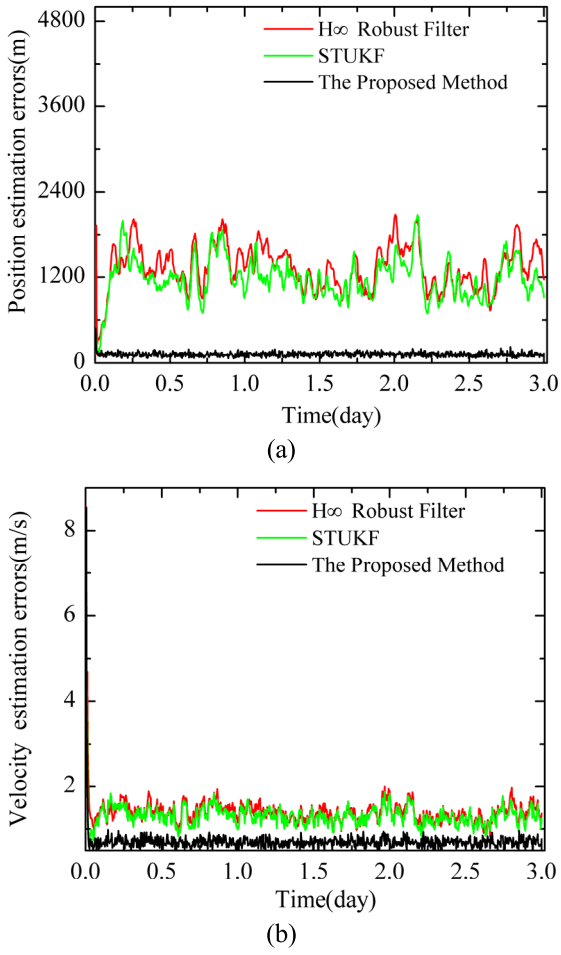

FIGURE 6. Position and velocity estimation errors in strong noise environment, (a) position estimation errors, (b) velocity estimation errors.

experiment, because that both strong noise and state model errors exist, the performances of H∞ robust filter and STUKF deteriorate seriously. Attributed to the estimation and correction of the state model errors and the introduction of fading factor, the proposed method has good robustness against noises and state model errors.

And then, we analyze the XPNAV filtering performance of the proposed method in the presence of state model errors. Here, we introduce saltatory state $\Delta \boldsymbol{X} = [0, 0, 0, 0, 2\ \mathrm{m/s^2}, 0]$ when $t \in (0.2 \cdot t_{obs}, 0.3 \cdot t_{obs})$, t_{obs} is the total observation time. And the actual state model of the spacecraft is changed to the following equation,

$$\boldsymbol{X}_{k+1} = \boldsymbol{f}(\boldsymbol{X}_k + \Delta \boldsymbol{X}_k) + \boldsymbol{w}_k \tag{35}$$

We still conduct the XPNAV experiment using the original state model mentioned in (8) and guarantee the same conditions to verify the effectiveness and robustness of the proposed method. Results are shown in Fig. 7 and Fig. 8.

Fig. 7 shows that the position estimation errors of H∞ robust filter and STUKF increase significantly when the spacecraft' state suddenly changes. And the estimation errors decrease when the spacecraft' state returns to normal. STUKF

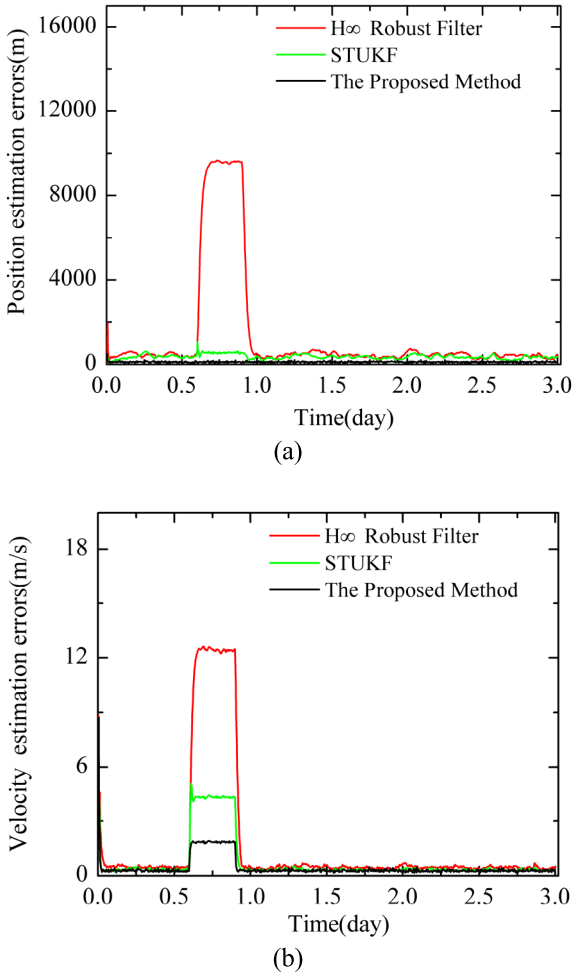

FIGURE 7. Position and velocity estimation errors in the presence of state model errors, (a) position estimation errors, (b) velocity estimation errors.(measurement period: 300s).

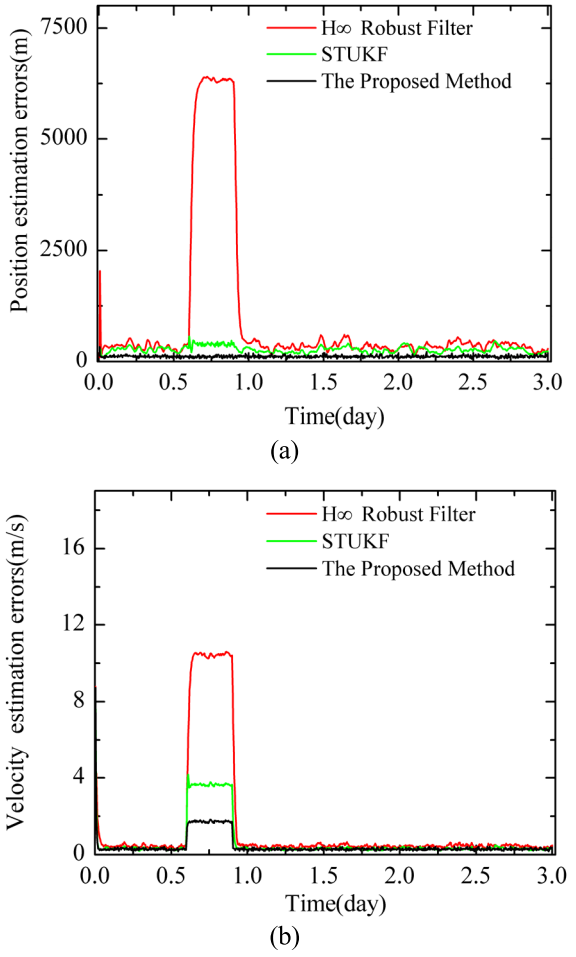

FIGURE 8. Position and velocity estimation errors in the presence of state model errors, (a) position estimation errors, (b) velocity estimation errors. (measurement period: 600s).

performs better than H∞ robust filter but still has large position estimation errors. It is noteworthy that the proposed method has strong robustness, excellent tracking capability and smaller position estimation errors when the spacecraft's state changes. Due to lack of the ability to estimate and correct the state model errors, the other two methods cannot track the spacecraft' state in real time and thus produce large state estimation errors once the spacecraft' state changes.

Fig.8 shows that the position and velocity estimation accuracy of the three method can be improved as the pulsar signal measurement period increases. Because that more pulsar signals are obtained with the increase of measurement period.

To verify the robustness of the proposed method in the presence of larger state model errors, we introduces saltatory state $\Delta \boldsymbol{X} = [0, 0, 0, 0, 20\ \mathrm{m/s^2}, 0]$ when $t \in (0.2 \cdot t_{obs}, 0.3 \cdot t_{obs})$, which is 10 times larger than the original state errors set in this paper. And conduct the XPNAV experiment and guarantee the same conditions. Results are shown in Fig.9.

Fig.9 shows that the larger state model errors lead to the larger position estimation errors of H∞ robust filter, STUKF and the proposed method.

And then, we analyzed the relationship between the position estimation accuracy and the pulsar signal measurement period in strong noise environment. The results are shown in Fig. 10.

From Fig.10 we can see that the position estimation errors of the three methods reduces as the pulsar signal' measurement period increases. And we can conclude that, under certain circumstances, the longer the measurement period is, the more pulsar signals will be received, the more accurate the calculation of navigation observations will be, and the higher the navigation accuracy will be. In addition, we can see that the proposed method performs best in that it has the smallest position estimation errors. This further proves the robustness, effectiveness and feasibility of the proposed method.

Finally, we conduct 400 Monte Carlo experiments for quantitative analysis of the position estimation accuracy of the three methods in different situations. The average position estimation errors are given in Tables 5

The results show when the initial position error of the spacecraft is [10 km, 10 km, 10 km] and the initial velocity error is [5 m/s, 5 m/s, 5 m/s] with a filter update time of 300 s

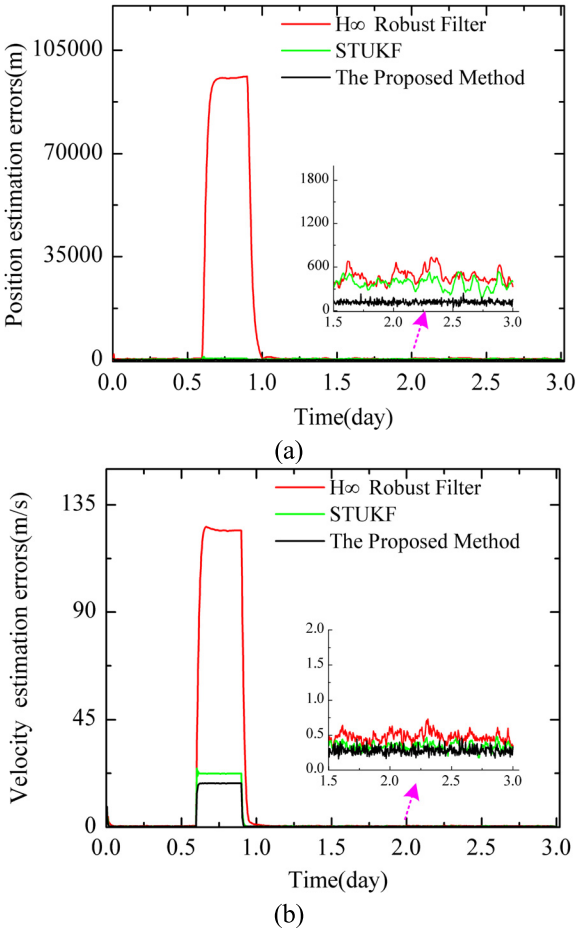

FIGURE 9. Position and velocity estimation errors in the presence of larger state model errors, (a) position estimation errors, (b) velocity estimation errors (measurement period: 300s).

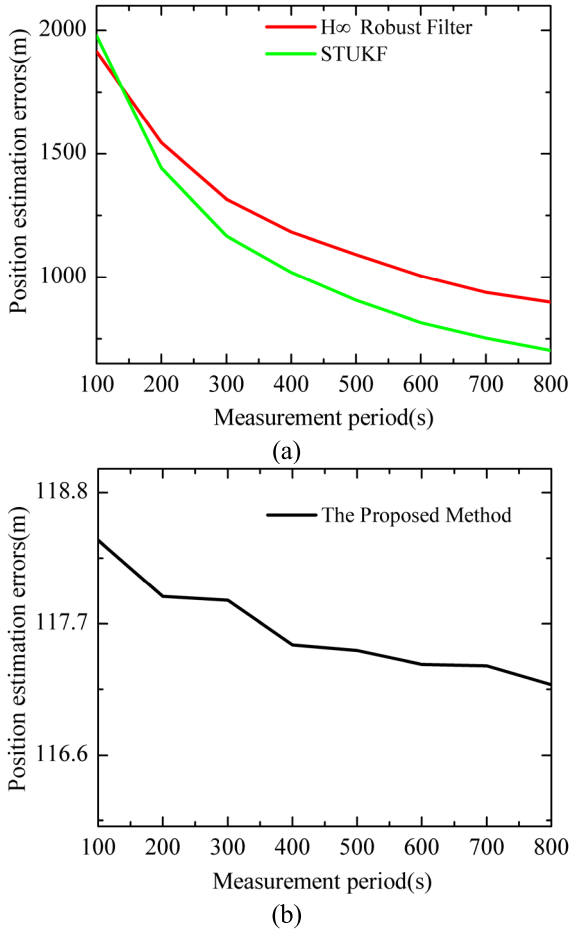

FIGURE 10. Accuracy of position estimation under different measurement periods in strong noise environment, (a) position estimation error of H∞ robust filter and STUKF, (b) position estimation errors of the proposed method.

TABLE 5. Position estimation errors for different situations.

Position estimation errors(m)				
Observation time/s	Method	Normal situation	Strong noises situation	In the presence of state model errors
300	H∞ robust filter	460.59	1291.7	1369.1
	STUKF	344.33	1169.0	364.69
	The Proposed Method	117.38	117.88	117.83

and a simulation time of 3 days, the navigation filtering accuracy of the proposed method is superior to the accuracies of H∞ robust filter and STUKF. In normal situation, a position estimation accuracy of 117.38 m can be achieved. With strong noise interference, a position estimation accuracy of 117.88 m can be realized. In the presence of state model errors, a position estimation accuracy of 117.83 m can be achieved. The results prove the robustness and superiority of the proposed method.

C. ANALYSIS AND DISCUSSION

The performances of the three methods used in XPNAV are then analyzed.

H∞ robust filter is a robust version of the Kalman filter [24]. It makes no assumption about the disturbances and introduces H∞ norm to minimize the estimation error of the system under the worst interference by minimized the H∞ norm of the error output. However, the optimal H∞ filtering problem is difficult to be solved to obtain the analytic form of the solution. By setting a constraint condition θ, the suboptimal H∞ filter can be achieved. Thus, the constraint condition θ has important influence on the filtering accuracy and robustness. The smaller the threshold is set, the stronger the robustness of this method is and the more serious the loss of filter accuracy is; The larger the threshold is set, the closer the characteristics of H∞ filter are to the standard Kalman filter. In this paper, in order to ensure the robustness of this method, the θ is set as fixed according to engineering practice experience, so that the filter performance has a certain conservative and cannot guarantee the estimation error is small even though the system is robust.

STUKF introduces a fading factor on the basis of UKF to realize the adjustment of the gain matrix and to force the residual sequence to be orthogonal in real time. Thus, the STUKF is more robust to noises and interferences than UKF. However, STUKF has no ability to correct the state model errors. When there are large state model errors and the incompletely orthogonal residual sequences, the estimation accuracy of STUKF will seriously reduce.

The proposed method uses state model errors and observation errors to construct a criterion function of state model error. By minimizing this criterion function, the errors of the system state model can be estimated. And the system state model can be corrected using the minimum state model error. Then, in order to predict the spacecraft' state of the next moment with high precision, the gain matrix is adjusted in quasi real-time by using the fading factor to ensure a minimized variance of the state estimation error and an orthogonal residual sequence at a different time. Thus, attributed to the estimation and correction of the state model errors and the introduction of fading factor, the proposed method has good robustness against noises and state model errors and can significantly improve the navigation accuracy in XPNAV.

V. CONLUSION

In this paper, we have proposed a robust navigation filtering method based on the advantages of the nonlinear prediction theory and strong tracking theory to reduce the serious effect of spacecraft' state model errors and strong noise on XPNAV. The performances of the proposed method have been compared with H∞ robust filter and STUKF. Experimental results of multi-group simulations show that the proposed method can significantly improve the accuracy of position and velocity estimation without increasing the computational complexity. And the accuracy of the proposed method is better than that of H∞ robust filter and STUKF, especially when the state model errors and noises are great. Thus, the proposed method is suited for spacecraft autonomous navigation and is available to estimate the spacecraft's state with high-precision in XPNAV.

The next phase of our research plan is to improve the proposed method by solving the problem of matrix nonsingularity which sometimes exists in this method. Then, based on the proposed method, the XPNAV enhancement technology by combining other methods and information will be researched to improve the accuracy of XPNAV navigation. In addition, extending this method to other robust control systems is also one of the directions of future research.

REFERENCES

[1] T. J. Chester and S. A. Butman, "Navigation using X-ray pulsars," Telecommun. Data Acquisition Prog. Rep. 63, Mar. 1981, pp. 22–25.
[2] S. I. Sheikh and, D. J. Pines, "Recursive estimation of spacecraft position and velocity using X-ray pulsar time of arrival measurements," *Navigation*, vol. 53, no. 3, pp. 149–166, Sep. 2006.
[3] S. I. Sheikh, D. J. Pines, P. S. Ray, K. S. Wood, M. N. Lovellette, and M. T. Wolff, "Spacecraft navigation using X-ray pulsars," *J. Guid., Control, Dyn.*, vol. 29, no. 1, pp. 49–63, Feb. 2006.
[4] J. Liu, J. Ma, J.-W. Tian, Z.-W. Kang, and P. White, "X-ray pulsar navigation method for spacecraft with pulsar direction error," *Adv. Space Res.*, vol. 46, no. 11, pp. 1409–1417, Dec. 2010.
[5] A. A. Emadzadeh and J. L. Speyer, "Relative navigation between two spacecraft using X-ray pulsars," *IEEE Trans. Control Syst. Technol.*, vol. 19, no. 5, pp. 1021–1035, Sep. 2011.
[6] J. Liu, Z. W. Kang, P. White, J. Ma, and J. W. Tian, "Doppler/XNAV–integrated navigation system using small-area X-ray sensor," *IET Radar, Sonar Navigat.*, vol. 5, no. 9, pp. 1010–1017, Dec. 2011.
[7] A. A. Emadzadeh and J. L. Speyer, "On modeling and pulse phase estimation of X-ray pulsars," *IEEE Trans. Signal Process.*, vol. 58, no. 9, pp. 4484–4495, Sep. 2010.
[8] Y. D. Wang, W. Zheng, S. M. Sun, and L. Li, "X-ray pulsar-based navigation using time-differenced measurement," *Aerosp. Sci. Technol.*, vol. 36, pp. 27–35, Jul. 2014.
[9] L.-R. Shen, X.-P. Li, H.-F. Sun, H.-Y. Fang, and M.-F. Xue, "A novel period estimation method for X-ray pulsars based on frequency subdivision," *Frontiers Inf. Technol. Electron. Eng.*, vol. 16, no. 10, pp. 858–870, Oct. 2015.
[10] M. Xue, X. Li, L. Fu, H. Fang, H. Sun, and L. Shen, "X-ray pulsar-based navigation using pulse phase and Doppler frequency measurements," *Sci. China-Inf. Sci.*, vol. 58, no. 12, pp. 1–14, Dec. 2015.
[11] J. Liu, J. Fang, J. Wu, Z. Kang, and X. Ning, "Fast non-linearly constrained least square joint estimation of position and velocity for X-ray pulsar-based navigation," *IET Radar, Sonar Navigat.*, vol. 8, no. 9, pp. 1154–1163, Dec. 2014.
[12] Y. Zhou, P. Wu, and X. Li, "Autonomous navigation for lunar satellite using X-ray pulsars with measurement faults," *IET Sci., Meas. Technol.*, vol. 10, no. 3, pp. 239–246, May 2016.
[13] A. A. Emadzadeh and J. L. Speyer, "X-ray pulsar-based relative navigation using epoch folding," *IEEE Trans. Aerosp. Electron. Syst.*, vol. 47, no. 4, pp. 2317–2328, Oct. 2011.
[14] L. B. Winternitz, M. A. Hassouneh, J. W. Mitchell, S. R. Price, W. H. Yu, S. R. Semper, P. S. Ray, K. S. Wood, Z. Arzoumanian, and K. C. Gendreau, "SEXTANT X-ray pulsar navigation demonstration: Additional on-orbit results," in *Proc. Int. Conf. Space Oper.*, Marseille, France, May 2018, pp. 1–10.
[15] H. Xia, Y.-H. Diao, G.-C. Ma, Z. Cao, and C.-H. Wang, "X-ray pulsar relative navigation approach based on extended Kalman filter," *J. Chin. Inertial Technol.*, vol. 22, no. 5, pp. 619–623, Oct. 2014.
[16] A. Giannitrapani, N. Ceccarelli, A. Garulli, and F. Scortecci, "Comparison of EKF and UKF for spacecraft localization via angle measurements," *IEEE Trans. Aerosp. Electron. Syst.*, vol. 47, no. 1, pp. 75–84, Jan. 2011.
[17] J. Liu, J. Fang, X. Ning, J. Wu, and Z. W. Kang, "Closed-loop EKF-based pulsar navigation for mars explorer with Doppler effects," *J. Navigat.*, vol. 67, no. 5, pp. 776–790, Sep. 2014.
[18] S. J. Julier and J. K. Uhlmann, "New extension of the Kalman filter to nonlinear systems," *Proc. SPIE*, vol. 3068, pp. 182–194, Jul. 1997.
[19] S. Julier, J. Uhlmann, and H. F. Durrant-Whyte, "A new method for the nonlinear transformation of means and covariances in filters and estimators," *IEEE Trans. Autom. Control*, vol. 45, no. 3, pp. 477–482, Mar. 2000.
[20] X.-P. Deng, J.-H. Zheng, and D. Gao, "Application research of modified unscented Kalman filter in X-ray pulsar navigation," *Trans. Beijing Inst. Technol.*, vol. 32, no. 1, pp. 51–55, Jan. 2012.
[21] X. Li, J. Jin, and Y. Shen, "Modified unscented Kalman filter for X-ray pulsar-based navigation system in the presence of measurement outliers," *Proc. Inst. Mech. Eng., G, J. Aerosp. Eng.*, vol. 232, no. 2, pp. 260–269, Feb. 2018.
[22] Z. Gen, Y. Yang, and X. Wen, "Strong tracking UKF method and its application in fault identification," *Chin. J. Sci. Instrum.*, vol. 29, no. 8, pp. 1670–1674, Aug. 2008.
[23] L. Sun, G. Y. Huang, and Y. Li, "Exploration of improved strong tracking SVD-UKF used in BDS/INS integrated navigation," *Comput. Eng. Appl.*, vol. 53, no. 10, pp. 225–229, 2017.
[24] D. Simon, *Optimal State Estimation: Kalman, H Infinity, and Nonlinear Approaches*. Hoboken, NJ, USA: Wiley, 2006, pp. 333–391.
[25] J. Liu, J. Ma, and J. W. Tian, "CNS/pulsar integrated navigation using two-level filter," *Chin. J. Electron.*, vol. 19, no. 2, pp. 265–269, Apr. 2010.
[26] J. Liu, "X-ray pulsar-based spacecraft autonomous navigation," Ph.D. dissertation, State Key Lab. Multi-Spectral Inf. Process. Technol., Huazhong Univ. Sci. Technol., Wuhan, China, 2011.
[27] Y. Wang, W. Zheng, S. Sun, L. Li, and X. L. Tan, "Autonomous navigation method for low-thrust interplanetary vehicles," *J. Aerosp. Eng.*, vol. 29, no. 1, pp. 04015009-1–04015009-9, 2015.

[28] K. Xiong, C. L. Wei, and L. D. Liu, "Robust multiple model adaptive estimation for spacecraft autonomous navigation," *Aerosp. Sci. Technol.*, vol. 42, pp. 249–258, Apr./May 2015.
[29] J. Jin, M. Wang, L. Huang, L. He, and Y. Jiang, "Study on the application of NPF algorithm in the X-ray pulsar navigation," *J. Astronaut.*, vol. 36, no. 11, pp. 747–753, Nov. 2015.
[30] Z. Guo, L. J. Miao, and H. S. Zhao, "An improved strong tracking UKF algorithm and its application in SINS initial alignment under large azimuth misalignment angles," *Acta Aeronautica Astron. Sinica*, vol. 35, no. 1, pp. 203–214, Jan. 2014.
[31] L. Huang, P. Shuai, X. Zhang, and S. Chen, "A new explorer mission for soft X-ray timing—Observation of the Crab pulsar," *Acta Astron.*, vol. 151, pp. 63–67, Oct. 2018.
[32] M. Xue, Y. Shi, Y. Guo, N. Huang, D. Peng, J. Luo, H. Shentu, and Z. Chen, "X-ray pulsar-based navigation considering spacecraft orbital motion and systematic biases," *Sensors*, vol. 19, no. 8, pp. 1877–1893, Apr. 2019.

LIRONG SHEN received the Ph.D. degree in test and measurement technology and instruments from Xidian University, China, in 2017.

She is currently a Lecturer with the School of Aerospace Science and Technology, Xidian University. Her main research interests include pulsar signal processing and its applications in navigation.

HAIFENG SUN received the M.S. and Ph.D. degrees from Xidian University, in 2011 and 2015, respectively.

He is currently an Associate Professor with the School of Aerospace Science and Technology, Xidian University, China. His research interests include celestial navigation and signal processing theory, and navigation signal processing technology.

XIAOPING LI received the Ph.D. degree from Xidian University, China, in 2004.

She is currently a Professor and the Dean of the School of Aerospace Science and Technology, Xidian University. Her research interests include information fusion, intelligent information processing, and information security.

YANMING LIU received the Ph.D. degree from Xidian University, China, in 2003.

He is currently a Professor and the Deputy Dean of the School of Aerospace Science and Technology, Xidian University. His research interests include the communication of the near space aircrafts, space-air ground information networks, and space physics characteristics.

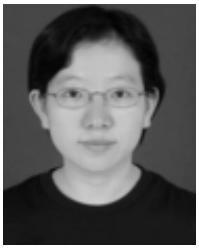

HAIYAN FANG received the Ph.D. degree in mechanical manufacturing and automation from the Xi'an University of Technology, in 2005.

She is currently an Associate Professor with the School of Aerospace Science and Technology, Xidian University, China. Her research interests include autonomous navigation and signal processing.

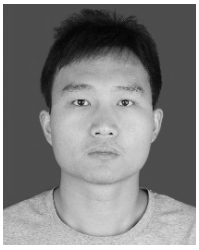

JIANYU SU is currently pursuing the Ph.D. degree with Xidian University.

His research interest includes pulsar signal processing.

LI ZHANG is currently pursuing the Ph.D. degree with Xidian University.

His research interest includes pulsar-based navigation.